PROCEEDINGS OF SCIENCE

A systematic theoretical study of explosion energies in Core Collapse Supernovae

Yu Yamamoto[*a], **Shoichi Yamada**[ab]

[a] *Department of Science and Engineering, Waseda University , 3-4-1 Okubo, Shinjuku, Tokyo 169-8555, Japan*

[a] *Advanced Research Institute for Science and Engineering, Waseda University, 3-4-1 Okubo , Shinjuku, Tokyo 169-8555, Japan*

E-mail: `yamamoto@heap.phys.waseda.ac.jp`

We suggest a new experimental approach to conduct a systematic study in core collapse supernovae (CCSNe) theory. We provide toy pre-supernova stages with controlled core and silicon sulfer (Si+S) layer masses solving NSE and QSE compostions respectively. We also demonstrated 1D hydrodynamic simulations with light bulb approximation using 6 models from core collapse to explosion in order to study the dependence of the interior structures of pre-supernova stages on both explosion energies and nickel masses.

During the core collapse our simulation showed that Si+S layer masses are most important in deciding the time evolution of mass accretion rates after bounce. We also found that the lighter core mass models produce the more energetic explosions and larger amounts of nickel masses. When the Si+S layer masses are lighter, mass accretion rates are enhanced so that the heavy core mass models are prevented from producing powerful explosions. Our simulation shows neccesity of early time explosion to reproduce 10^{51} erg .

XIII Nuclei in the Cosmos,
7-11 July, 2014
Debrecen, Hungary

*Speaker.

PoS(NIC XIII)176

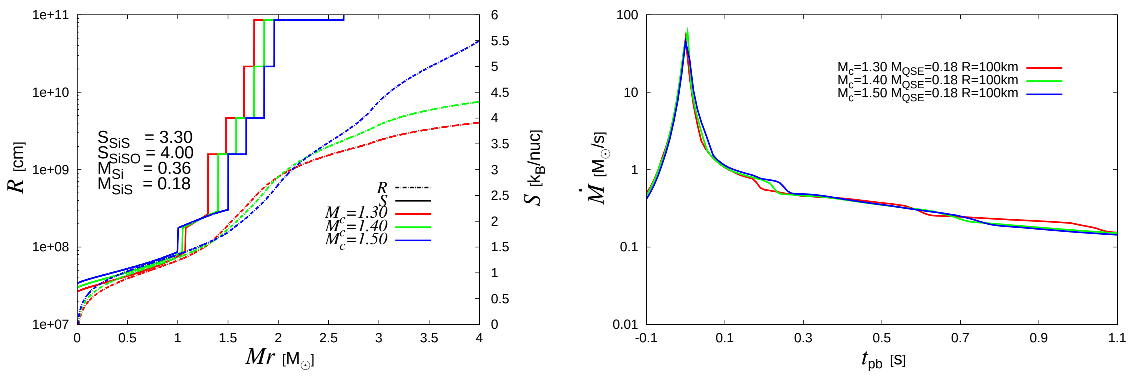

Figure 1: The left panel : Entropy (solid line) and radius (dashed line) profiles as functions of enclosed mass for the different core mass progenitors, $M_c = 1.30$ (blue line), 1.40 (red line) and 1.50$M_\odot$ (green line) respectively. The Si+S layer mass are fixed to 0.18$M_\odot$. The right panel : Time evolutions of mass accretion rate, $\dot{M}$, at 100 km for the same models in the left panel. The origin is taken at the times when each $\dot{M}$ took peak values in each model.

1. Introduction

Just like the neutron star merger scenario has remarkably succeeded in explaining r-process nucleo synthesis, core collapse supernovae (CCSNe) are considered as one of the most likely sites to produce heavy elements [6]. However, we remind that the canonical explosion [3], $E_{exp} \gtrsim 10^{51}$[erg] and $M_{Ni} \lesssim 0.10 M_\odot$, has not been obtained by the state-of-art simulations yet. Recent studies show a wide divergence in CCSNe fates even for modest mass difference in progenitors [9] [2]. It is well known that even for same zero-age main sequence (ZAMS) masses and metallicities, the results from different stellar evolution code do not agree with each other [1].

Our aim is to make clear the necessary conditions to generate the energetic explosions. For the first step, we made toy models of pre-supernova stage progenitors with controlled core and Si+S layer masses to investigate the dependence of the progenitor interior structures on the explosion energy and nickel mass. This experimental method would give some important clues to understand what kind of properties are essential to reproduce the observed E_{exp} and M_{Ni}. We describe briefly how we construct our toy models in the next section.

2. Setup & Methods

2.1 Toy pre-supernova stages

We found interesting characteristics of presupernova stage progenitors in Woosley et al. (2002)[8]. Entropy and electron fraction (Ye) of inside the core of massive stars seem to correlate with density. Under these entropy/Ye-density empirical relations inside the central core, we solved the mass conservation and hydrostatic equations and constructed pre-supernova stage models with more than 10 parameters. Since our aim is to see the dependence of core masses on explosion energies and nickel masses, we construct 6 "toy" pre-supernova models with 3 different core masses ($M_c = 1.30, 1.40, 1.50\mathrm{M}_\odot$) and 2 different Si+S layer masses($M_{SiS} = 0.09, 0.18\mathrm{M}_\odot$). We set the entropies inside each layers to be constant, i.e. distributed as a step fuction. (see the left panel of Fig. 1). We also assume that the composition of the core is in nuclear statistical equilibrium (NSE), those of Si+S layer as quasi statistical equilibrium (QSE) and those of other envelopes as fixed values. The left panel of Fig. 1 show various $R - M_r$ relations obtained by this experimental method. The result show that we could produce models with various 'compactness'[4], which is consider to be an important factor in CCSNe theories.

2.2 1D dynamical simulation and steady shock solution

We carried out spherical hydrodynamical calculations including chemical abundance evolution and excluding central part of stars. For every model we separate the whole process into 3 steps, 1) core collapse 2) steady shock and 3) shock revival and explosions, to determine both explosion energies and nickel masses. The 2nd step is necessary to construct the initial condition of the 3rd step. We employ the light bulb approximation, a parameteric neutrino luminosity method, for the 2nd and 3rd steps. The method of calculation is similar to our previous work [10] but the derivation of critical neutrino luminosities are different. Instead of fixing the mass accretion rates, we let them evolve and leave the calculation until the mass accretion rates get sufficiently low to explode under the constant luminosity which we choose $L_\nu = 2.5 \times 10^{52}\mathrm{erg/s}$. We defined the onset of explosion as when the diagnostic explosion energy exceeds 10^{48}erg. The time dependence of each PNS property, L_ν, T_ν and r_ν, are unchanged from our previous work. We terminate the simulation when shock radii reaches $r_{sh} \sim 1.5 \times 10^9$cm.

Another major advance is the improvement of input physics. To calculate chemical compositions more precisely, 297 nuclei ($Z \leqq 32$) are assumed to reach NSE when $T_9 > 7.0$. Below $T_9 = 7.0$, we solved nuclear reaction network for 28 nuclei and the remaining 269 nuclei are average to a single “virtual” heavy element so that we can connect NSE regions to non-NSE regions consistently even in small Ye situations. We used Reaclib data [5] for calculating reaction rates. The dominant nuclear reactions are (α, γ), (p, γ) and their inverses in our simulation.

3. Results

3.1 Collapse

The history of mass accretion rates first show monotonic decrease after large peaks. Such character is also reported in Buras et al. (2006)[1] where the mass accretion rates peaked at the moment of core bounce. From this point of view we defined our peak mass accretion time as 'core bounce' time, $t_{pb} = 0$ms. We found that the difference in Si+S layer masses have a large impact on the mass accretion rate history. For example see the right panel of Fig. 1. When we take the origin at core bounce times, the mass accretion rates follow very similar evolutions up to $t_{pb} = 700ms$, for fixed M_{SiS}. There are, however, slight differences due to the locations of Si+S/Si+S+O interface and Si/O interface. We also confirmed that after $t_{pb} = 300$ms, radial distributions of $\dot{M}$ were uniform interior to 500km in each model and applied these snapshots to construct the steady shock solutions in step 2.

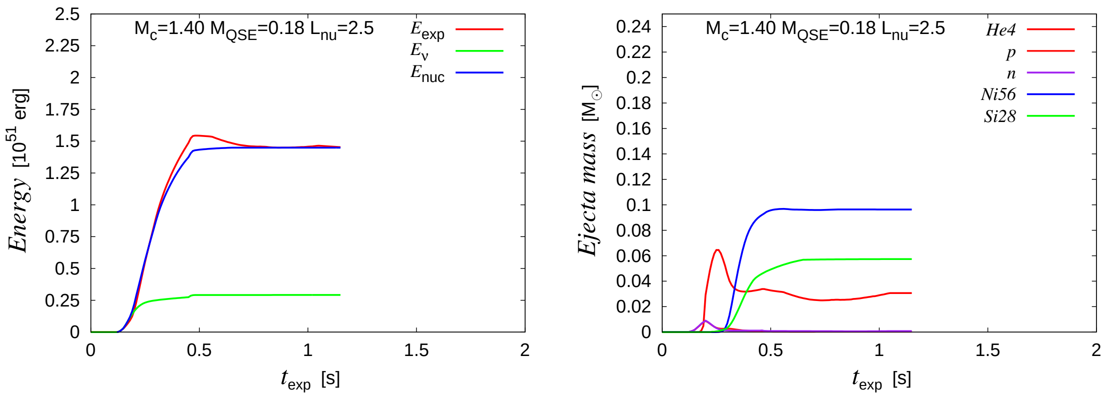

Figure 2: The left panel : The time evolutions of a diagnostic explosion energy (red line), total nuclear energy release(blue line) and neutrino heating energy (green line). The right panel : The time evolutions of α (red line), ^{56}Ni (blue line), ^{28}Si (green line), proton (megenta) and neutron (purple). The model is $M_c = 1.40\mathrm{M}_\odot$ with $M_{SiS} = 0.18\mathrm{M}_\odot$ and neutrino luminosities are set to $L_\nu = 2.5 \times 10^{52}\mathrm{erg/s}$.

3.2 Shock revivals & Explosion

Starting from $t_{pb} = 300\mathrm{ms}$ with $L_\nu = 2.5 \times 10^{52}\mathrm{erg/s}$, all 6 models show a successful shock revival. As the qualitative time evolutions of explosion energy and nickel mass are similar to each other, we only discuss the fiducial model, namely $(M_c, M_{SiS}) = (1.40\mathrm{M}_\odot, 0.18\mathrm{M}_\odot)$. The time evolution of explosion energy and two important source energies are drawn in Fig.2. From the left panel of Fig. 2 the explosion energy first increased by nuclear energy release and neutrino heating and then decreased by swallowing gravitationally bound envelopes. Their time evolution behave similar to the energy release from the nuclear binding energies. The energy components were integrated only over radially expanding and unbounded matter. On the other hand, the right panel of Fig. 2 show the time evolutions of different ejecta. You could easily see the chain recombination from nucleon to nickel at $150ms \lesssim t_{exp} \lesssim 500ms$. After $t_{exp} = 300\mathrm{ms}$, α rich freeze-out occurs because the temperature drops below $T_9 = 3.0$. The nuclear timescale is much longer than the dynamical timescale. It took about 600ms to reach saturation of both energy and ejecta mass from the onset of explosion when $E_{exp} \gtrsim 10^{51}\mathrm{erg}$. These results are similar to our previous work [10].

Table. 1 show the final results of the 6 models. Powerful explosions were generated in $M_c = 1.30$ and $1.40\mathrm{M}_\odot$ models. This is due to the weaker gravitational energies which leads to higher $\dot{M}$ explosion compared with $M_c = 1.50\mathrm{M}_\odot$. The different Si+S layer masses result in almost the same M_{PNS}, which correspond to the same explosion onset, but different M_{Ni} by 20%. This means that not the core mass but the Si+S layer masses affect the result of M_{Ni}, namely stronger $\dot{M}$ produce larger nickel masses. When it comes to the heavy core mass models, $M_c = 1.50\mathrm{M}_\odot$, the situation is altered because of different explosion times. The magnitude of the neutrino luminosity is not sufficient in this case so that we have to wait for explosion until $\dot{M}$ drops to a certain value. The mass accretion flow increase the PNS mass and weaks the explosion drastically. Although we had

M_c [$M_\odot$]		E_{exp} [10^{51}erg]		M_{Ni} [$M_\odot$]		M_{PNS} [$M_\odot$]	
	M_{SiS}[$M_\odot$]	0.09	0.18	0.09	0.18	0.09	0.18
1.30		1.64	1.40	0.149	0.124	1.532	1.519
1.40		1.43	1.45	0.122	0.096	1.628	1.614
1.50		0.73	1.07	0.084	0.094	1.815	1.731

Table 1: The explosion energies, E_{exp}, M_{Ni} and M_{PNS} for all 6 models. The neutrino luminosities in all models are set to $L_\nu = 2.5 \times 10^{52}$erg/s at the start of simulations.

4 powerful explosion models, only one fiducial model is found among our toy models because of too large nickel yields. We expect, however, that this nickel overproduction would be buffered in multi-dimensional simulations due to fall back effects.

4. Summary

We performed a systematic theoretical study of E_{exp} and M_{Ni} by constructing toy pre-supernova stage models and conducting 1D spherical hydrodynamic simulations. As our aim is to see the relation between the interior structure of the progenitor and E_{exp} and M_{Ni}, we focused on only changing 2 parameters, core mass and Si+S layer mass, and fixed other parameters to provide pre-supernova stage models in this work. This experimental approach can cover a large range of compactness. The Si+S layer masses play an important role on the M_r-R relation, thus affecting mass accretion rates. Because of the smaller gravitational energy, $M_c = 1.30$ and $M_c = 1.40M_\odot$ showed "earlier" shock revival at hirher $\dot{M}$ stages and energetic explosions. "Early time" explosion seems to be essential to provide $E_{exp} \sim 10^{51}$erg. In the models with same explosion time, nickel masses were lower for the heavier Si+S mass models due to lower $\dot{M}$.

References

[1] Buras, R., Janka, H.-Th., Rampp, M., Kifonidis, K. 2006, A&A, 457, 281

[2] Nakamura, K., Takiwaki, T., Kuroda, T., Kotake, K., arXiv:1406.2415

[3] Nomoto, K., Tanaka, M., Tominaga, N., Maeda, K., 2010, NewAR, 54, 191

[4] O' Connor, E., & Ott, C. D. 2011, ApJ, 730, 70

[5] Rauscher, T., & Thielemann, F.-K. 2000, Atomic Data and Nuclear Data Tables, 75, 1

[6] Roberts, L. F. 2012, ApJ, 755, 126

[7] Sukhbold, T., & Woosley, S. E. 2014, ApJ, 783, 10

[8] Woosley, S. E., Heger, A., & Weaver, T. A. 2002, Reviews of Modern Physics, 74, 1015

[9] Ugliano, M., Janka, H.-Th., Marek, A., Arcones, A., 2012, ApJ, 757, 69

[10] Yamamoto, Y. , Fujimoto, S.-i., Nagakura, H., & Yamada, S. 2013, ApJ, 771, 27